Reviewer 1 Comments

Reviewers Comment (RC) 1: This contribution is unique and important for the society of research and development on the image-based hydrometry approach. Provided images are useful for the RD mentioned above. Other than images, information for validation is described in the manuscript. The unfortunate thing is that quantitative validation data was not included in the provided data set. This restricts the aim of this contribution, "validation and accuracy assessment" (the last sentence in an abstract.) To accomplish the objective of the study further, I suggest some modifications in both the manuscript and the dataset.
Authors Comment (AC) 1: Thanks for the considered review of our submitted article. In response to comments from reviewers 1, 2 and 3, the revised version of the manuscript now fully describes the validation data available for each of the case studies. This validation data has been collated and published in the data archive along with the orthorectified images.

RC 2: Lines 11-14, page 2: Two sentences are discussing the image velocimetry application in labs and the logical flow between two sentences is difficult to follow. To make this part easier for reading, one option is to move "wide variety of experimental conditions" at the beginning part of the second sentence, since this part is a distinguishing point to the first sentence
AC 2: The sentences in question has been revised to read: 'Image velocimetry involves the application of cross-correlation, or computer vision techniques on a series of consecutive images (or extracted video frames) to generate vectors of water velocities across a field-of-view. It was originally developed for use in highly controlled laboratory settings. However, since its original conception, its application has expanded from use in the laboratory (e.g., Dudderar and Simpkins, 1977; Adrian, 1984; Pickering and Halliwell, 1984), to include a wide variety of experimental conditions.'

RC 3: Figure 1. I suggest dropping "Geographical" from the caption or add some more information regarding geography in the figure, e.g. water network, river basin, elevation, etc.
AC 3: The Figure caption has been modified to read: 'Locations of the monitoring sites from which data is presented. Numbers correspond with the in-text subsections: (1) River Arrow, UK; (2) River Thalhofen, Germany; (3) Murg River, Switzerland; (4) Alpine River, Austria; (5) River Brenta, Italy; (6) La Morge, France; (7) St-Julien torrent, France; (8) River La Vence, France; (9) River Tiber, Italy; (10) River Bradano, Italy; (11) River Noce, Italy. Not shown: (12) Castor River, Canada; (13) Salmon River, Canada. Map spatial reference: ETRS (1989).'

RC 4: Figures 2 and 3. Original and rectified images are provided in each figure and I guess the directions are rotated. Better to indicate the direction of the flow, e.g. by putting the arrow with a label of "flow" onto each panel.
AC 4: For both Figures 2, 3, and 4, the flow direction has been indicated using an arrow along with the word 'Flow'.

RC 5: Table A2. Label, this is quite a minor thing but I suggest use "Image Aquisition" instead of "Data Aquisition" in the label.
AC 5: The label of Table A2 has been modified to read: 'Image Acquisition'.

RC 6: Table A2. Validation data, I suggest to add the description about validation data (e.g. how and where).

AC 6: In order to support the presentation of the validation data we have used this part of the table to provide a summary of the reference measurements undertaken for each case-study (e.g. instrument, number of points, location, etc.).

RC 7: Table A2. Flow information, I suggest adding the mean velocity, representative depth, Froude number, width etc. (maybe, rotate 90 degrees the table to expand the width of the table).
AC 7: Unfortunately, this information is not readily available for all the case-studies. However, we will have ensured that all relevant information describing the hydrological conditions for each case-study is presented within each sub-section of the text.

RC 8: Data-set. Better to include movie file for each site for making easier to know the image characteristics and image recording approaches. (I made by myself for the purpose of review, and I can share it if needed.) Also suggested is providing text file(s) specifying the image resolution, location of the edges of images, and frame rate, and/or provide e.g. jgw, tfw and pgw files for corresponding image/folder (for jpg, tiff and png image, respectively).
AC 8: Videos consisting of the orthorectified imagery has been provided in the Data Archive. These videos have been produced at the same image resolution as the orthorectified/stabilised images. This information is provided in the Readme.txt associated with each case study within the Data submission. Unfortunately, the geographical coordinates are unknown for many of the image sequences presented. In most cases, the ground control points were surveyed using an instrument that utilises a local reference (e.g. total station). In these cases, it would be inappropriate to provide a tgw, tfw, etc. file.

RC 9: Data-set. For sites with velocity distribution measured for validation, provide the location and velocity of the data as e.g. CSV file.
AC 9: The revised submission now includes reference velocity measurements for each of the case studies where it is available. This validation data has been collated and published in the data archive along with the orthorectified images. The locations of the velocity measurements are provided in pixel units based on the orthorectified images.

RC 10: Data-set. Type of image file and the structure of file name differ for each folder, this making the pre-processing a bit troublesome for a potential user of the data. Could you provide also a unified formatted image set, e.g. 0000.png? (I made this also by myself for review, and I can share it if needed.)
AC 10: The filenames have been altered and are now presented in a standardised format e.g. 00001.png.

Reviewer 2 Comments

RC 1: The present manuscript is aimed to introduce the new dataset, which will help to systematize and benchmark the emerging techniques for image-based river surface velocity estimation. The corresponding dataset consists of pre-processed videos from 12 research sites located in six different countries and covered a wide range of fluvial settings. In my opinion, the introduced dataset has sound potential and of high interest in the research community. However, I recommend authors to provide major revisions which may help to increase the dataset value for the target community and make it the first benchmark dataset for image-based velocimetry techniques (e.g., as the MNIST database for image classification).
AC 1: We would like to thank the reviewer for taking the time to provide a thorough review of our submitted manuscript.

RC 2: Abstract (Page 1, Ln 10): It is mentioned that 13 case studies have been presented in the dataset, but Section 2 describes only 12.
AC 2: 13 case studies are now presented and the abstract now reads: 'Reference data is available for 12 of the 13 case studies presented enabling these data to be used for reference and accuracy assessment.'

RC 3: Section 2.7 St-Julien torrent, France (Page 8, Ln 24-31): As for this particular case study, the validation data is unavailable, the explicit description is needed to clarify the reasons behind the inclusion of the corresponding data to the introduced dataset. At least, it is not clear how this data will help to pursue one of the dataset objectives as "testing specific image velocimetry techniques."
AC 3: This particular case study represents a flash flood, which occurred in a torrent system in Italy producing mean velocities of approx. 6 m s^{-1}. Whilst no reference measurements are available for this example, image velocimetry techniques perhaps offer the best opportunity to estimate flows under these extreme conditions. Researchers interested in reconstructing flash flood processes may find it valuable to understand how the range of available methods perform relative to each other, and software developers may find it instructive to consider how newly developed techniques compare with existing approaches under a diverse range of flow conditions. This justification has been provided in the manuscript.

RC 4: Section 2.9 River Tiber, Italy (Page 10, Ln 13-24): In my opinion, the single measurement of average velocity, which is provided as validation data for this site has limited value for the comprehensive analysis of different image velocimetry techniques reliability and efficiency. Please, provide explicit reasoning why this data will also help to meet the declared dataset objectives.
AC 4: Whilst only a single reference velocity value is available for the Tiber case-study, this measurement is representative of the surface velocities within an area of approx. 3 x 3m. The RVM20 speed surface radar system measurements can be compared with outputs derived from image velocimetry analysis within the 3 x 3m footprint. This justification has been provided in the manuscript.

RC 5: Dataset: I have realized that for some sites (e.g., Arrow River, Bradano River), scenes are not aligned with each other, i.e., ground (riverbanks) is not stable. In my opinion, key point alignment is needed to simplify the use of the dataset. This way, if the ground is stable for all the scenes, optical flow techniques can be easily implemented out-of-the-box for velocity field estimation.
AC 5: We acknowledge that the original submission of image sequences for the Arrow River and Bradano River case-studies were not stabilised. In the revised submission we have included both the stabilised and original images. We have chosen to include the un-stabilised footage as stabilisation is one of the critical challenges of using mobile platforms for image velocimetry analysis and the preferred approach may vary from researcher-to-researcher. Differences in the stabilisation technique may also have implications on the subsequent velocity outputs.

RC 6: Dataset: I recommend authors to consider the change of format for the provided images to GeoTIFF (or similar) to provide explicit georeferencing capabilities. It will substantially simplify the validation procedure by providing a solid basis for validation data georeferencing.
AC 6: Unfortunately, the geographical coordinates are unknown for many of the image sequences presented. In most cases, the ground control points were surveyed using an instrument that utilises a local reference (e.g. total station). Therefore, georeferencing of the images is problematic.

However, the reference velocity data has been provided in pixel units to ensure that comparisons between image velocimetry outputs and reference measurements should be straightforward.

RC 7: Dataset: I did not find any validation data mentioned in the manuscript (Section 2) in the provided dataset archive.
AC 7: The revised version of the manuscript now fully describes the validation data available for each of the case studies. This validation data has been collated and published in the data archive along with the orthorectified images, which were presented in the original submission.

RC 8: Dataset: In my opinion, the additional section, which will confirm the introduced dataset validity and its corresponding value for the target community, is needed. The potential reader has to be sure that the dataset is consistent with the declared objectives and therefore serves the reader's needs the best (e.g., benchmarking the new technique/software). I recommend authors to provide a brief analysis of the single case study showing the extracted velocities and comparing them to the validation data. Authors also may consider supporting the corresponding analysis with a code example - this may significantly increase the reader's interest to the dataset and manuscript itself.
AC 8: Analysis of the datasets provided is beyond this scope of this Data Description paper but we invite the reviewer to explore the references cited within the sub-section of each case-study and Table A2 as the datasets presented within this manuscript have been utilised to generate flow velocity data in previous published work.

Reviewer 3 Comments

RC 1: I think that the work is valuable and interested in the hydrology community for the development of image-based techniques, which could be further applied in modeling and monitoring.
AC 1: We would like to thank the reviewer for taking the time to assess the suitability of this manuscript to be published in Earth System Science Data, and for the constructive comments provided.

RC 2: However, it is not clear to me what contributions this paper offers. The abstract mentions inter-comparison and validation of the various techniques, but they were not actually performed, which seems to be missing a major component of the paper.
AC 2: The purpose of this manuscript is to introduce datasets that can be used for inter-comparison and validation of various techniques, rather than to perform inter-comparisons. This is beyond the scope of a Data Description paper. However, we invite the reviewer to explore the references cited within the sub-section of each case-study and Table A2 as the datasets presented within this manuscript have been utilised to generate flow velocity data in previous work.

RC 3: Abstract (Page 1, Ln 10): It is mentioned that 13 case studies have been presented in the dataset, but Section 2 describes only 12.
AC 3: This was a typographical error. However, we have since added an additional case-study. Therefore, we keep the text as it was in the original manuscript.

RC 4: The validation data exists for most cases, then why not present the resulting datasets in the form that is directly compared and validate, instead of the image clips?

AC 4: The revised version of the manuscript now fully describes the validation data available for each of the case studies. This validation data has been collated and published in the data archive along with the orthorectified images.

RC 5: Even if quantitative validation is addressed, the measurements are taken at specific time and location of the river (i.e. specific hydro-geomorphic setting), so it may not be comparable if someone uses different camera and processing technique at different time and/or location. I understand that the nature of the observation and approach is not suitable for generalization, but the paper in the current form doesn't seem to fit into the context of "towards harmonization of the techniques"
AC 5: The purpose of our approach is indeed specific to a particular instance and location within the river. By ensuring that images are acquired at the same time (or river stage) as the reference measurements, a comparison between the two approaches will be possible. Furthermore, this database seeks to present examples from a range of hydro-geomorphic settings, which will enable researchers to assess the suitability of their chosen approach under hydrological conditions that are of particular interest to them.

Towards harmonization of image velocimetry techniques for river surface velocity observations

Matthew. T. Perks[1], Silvano Fortunato Dal Sasso[2], Alexandre Hauet[3], Elizabeth Jamieson[4], Jérôme Le Coz[5], Sophie Pearce[6], Salvador Peña-Haro[7], James Bomhof[4], Salvatore Grimaldi[9,10], Alain Goulet[4], Borbála Hortobágyi[1], Magali Jodeau[11,12], Sabine Käfer[13], Robert Ljubičić[14], Ian Maddock[6], Peter Mayr[15], Gernot Paulus[8], Lionel Pénard[5], Leigh Sinclair[4], and Salvatore Manfreda[16]

[1]School of Geography, Politics and Sociology, Newcastle University, Newcastle upon Tyne, United Kingdom.
[2]Department of European and Mediterranean Cultures: Architecture, Environment and Cultural Heritage (DiCEM), University of Basilicata, 75100 Matera, Italy.
[3]Electricité de France, DTG, Grenoble, France.
[4]National Hydrological Services, Environment and Climate Change Canada.
[5]INRAE, UR RiverLy, River Hydraulics, Villeurbanne, France.
[6]School of Science and the Environment, University of Worcester, Worcester, UK.
[7]Photrack AG: Flow Measurements, Ankerstrasse 16a, 8004 Zürich, Switzerland.
[8]School of Geoinformation, Carinthia University of Applied Sciences, 9524 Villach, Austria.
[9]Department for Innovation in Biological, Agro-food and Forest Systems, University of Tuscia, Viterbo, Italy.
[10]Department of Mechanical and Aerospace Engineering, Tandon School of Engineering, New York University, Brooklyn, NY, United States.
[11]Electricité de France, R&D, Chatou, France
[12]LHSV, Chatou, France.
[13]Verbund Hydro Power GmbH, 9500 Villach, Austria.
[14]Faculty of Civil Engineering, University of Belgrade, Belgrade 11120, Serbia.
[15]flussbau iC, 9500 Villach, Austria.
[16]Department of Civil, Architectural and Environmental Engineering, University of Naples Federico II, Via Claudio 21, 80125 Napoli, Italy.

Correspondence: Matthew T. Perks (matthew.perks@newcastle.ac.uk)

Abstract. Since the turn of the 21st Century, image based velocimetry techniques have become an increasingly popular approach for determining open-channel flow in a range of hydrological settings across Europe, and beyond. Simultaneously, a range of large-scale image velocimetry algorithms have been developed, equipped with differing image pre-processing, and analytical capabilities. Yet in operational hydrometry, these techniques are utilised by few competent authorities. Therefore, imagery collected for image velocimetry analysis, along with ~~validation~~ reference data is required both to enable inter-comparisons between these differing approaches and to test their overall efficacy. Through benchmarking exercises, it will be possible to assess which approaches are best suited for a range of fluvial settings, and to focus future software developments. Here we collate, and describe datasets acquired from ~~six~~ seven countries across Europe and ~~Asia~~North America, consisting of videos that have been subjected to a range of pre-processing, and image velocimetry analysis ~~(Perks et al., 2020, https://doi.org/10.4121/uuid~~ ~~. Validation~~ (Perks et al., 2020, http://doi.org/10.4121/uuid:014d56f7-06dd-49ad-a48c-2282ab10428e). Reference data is available for 12 of the 13 case studies presented enabling these data to be used for ~~validation~~ reference and accuracy assessment.

1 Introduction

When designing hydrological monitoring networks, or acquiring opportunistic measurements for determining open-channel flow, the optimum choice of apparatus is likely to be a compromise between the data requirements, resource availability, and the hydro-geomorphic characteristics of the site (Mishra and Coulibaly, 2009). Generally, hydro-geomorphic factors will include: channel width and depth, the range of flow velocities, presence of secondary circulation, and cross-section stability. Each field measurement technique will have a designed range of optimum operating conditions, under which, robust flow measurements should be expected (e.g. ISO 24578:2012). However, under conditions beyond their designed operating range, greater levels of uncertainty will ensue. This may therefore preclude certain approaches for deployment under very shallow, or flood flow conditions for example. Logistical and practical constraints may also limit the deployment of apparatus. For example, techniques that require the device to be in contact with the water during operation may not be feasible for health and safety reasons during periods of high-flow, or due to staff availability (Harpold et al., 2006). As a result of some of these challenges, the potential for implementing alternative, non-contact approaches has been recently explored. Within this field of research, image velocimetry has emerged as an exciting new approach for determining a key hydrological characteristic, namely flow velocity.

Image velocimetry involves the application of cross-correlation, or computer vision techniques ~~to~~ on a series of consecutive images (or extracted video frames) to generate vectors of water velocities across a field-of-view. It was originally developed for use in highly controlled laboratory settings. However, since its original conception, its application has expanded from use in the laboratory (e.g., Dudderar and Simpkins, 1977; Adrian, 1984; Pickering and Halliwell, 1984), to include a wide variety of experimental conditions. Most notably it has been deployed outside of the controlled environment of the laboratory and into the domain of the field scientist (e.g., Fujita et al., 1998). It is now applied in complex environments including situations where lighting is not controlled, the camera platform may be mobile (e.g. on unmanned aerial systems (UAS)), images may be acquired oblique to the direction of flow, and at an angle that changes over time (e.g. Detert and Weitbrecht, 2015; Tauro et al., 2016b; Perks et al., 2016).

This technique is also becoming increasingly popular with the wider hydrological community (Tauro et al., 2018a), and this has been aided by two key factors. The first of which is the development of platforms and hardware that enable high-definition images and videos to be captured precisely, stored, and transferred to locations where image processing can occur. Secondly, many researchers utilizing image velocimetry techniques have chosen to develop their own specific processing capabilities, leading to the development of a range of both open-source and proprietary software for image pre-processing, and velocimetry analysis (Table A1). Whilst this has led to a breadth of options for researchers conducting image velocimetry analysis, inter-comparisons of their efficacy under a range of environmental settings, and flow regimes is currently lacking (Pearce et al., 2020) . Therefore, there is an urgent need to comprehensively understand and appreciate limitations of the differing image velocimetry approaches that are available to the scientific community.

Here, we present a range of datasets that have been compiled from across ~~six~~ seven countries in order to facilitate these inter-comparison studies (Figure 1, Perks et al. (2020)). These data have been independently produced for the primarily purposes of: (i) enhancing our understanding of open-channel flows in diverse flow regimes; and (ii) testing specific image velocimetry techniques. These datasets have been acquired across a range of hydro-geomorphic settings, using a diverse range of cameras, encoding software ~~, controller units, and with river velocity measurements generated as a result~~ and controller units. Image sequences have then been subjected to a range of differing image pre-processing ~~and~~ steps using a range of image processing software.

2 Experimental Design

Given the range of image velocimetry techniques that have been developed in recent years, benchmarking datasets covering a range of hydro-geomorphic conditions and acquisition platforms are required in order to test the accuracy and precision of each algorithm for the determination of 1- and 2-dimensional surface velocities. The examples that we describe in this section have been acquired by a range of platforms including UAS, fixed and hand-held cameras. The geographical characteristics of the sites are also widely varied. Catchment areas span $20–17\,460\,\mathrm{km}^2$, captured channel widths range from 5–~~28 m~~$59\,\mathrm{m}$, minimum flow depth is ~~0.22 m~~$0.10\,\mathrm{m}$, with a maximum of over $7\,\mathrm{m}$, and mean flow velocities range from ~~0.3~~ 0.13 to over $6\,\mathrm{m\,s^{-1}}$. Where possible, ~~validation~~ reference data generated by established and widely accepted approaches (e.g. ~~electromagnetic~~ current meter, and acoustic Doppler current profiler (ADCP)) have been collected simultaneously, or at the same river stage as images are acquired. The details pertaining to the hydrological conditions of deployment, configuration of the camera setup, pre-processing of imagery, and where relevant, details of published results from these datasets are presented in the following sections and summarised in Table A2.

2.1 River Arrow, UK

On 1st November 2017, a field experiment was undertaken on the River Arrow in Warwickshire (UK), to ascertain the accuracy of two differing image velocimetry approaches. The location of this experiment was in the mid-reaches of the catchment with a contributing area of ~~$319\mathrm{km}^2$~~$94\,\mathrm{km}^2$. This is a stable, meandering section of the river with an approximate width of $5\,\mathrm{m}$. During the experiment, mean depth and velocity were $0.22\,\mathrm{m}$ and ~~$0.42\mathrm{m\,s^{-1}}$~~ respectively and water turbidity was minimal with the gravel bed being ~~distinctly~~ clearly visible in the footage. The two deployments differed as both fixed ~~and mobile~~ (bankside pole-mounted) and mobile (UAS) imaging systems were used. Footage acquired from these two systems was captured concurrently, permitting direct comparisons to be made between the two. The mobile imaging system consisted of a DJI Phantom 4 Pro UAS equipped with a 1" camera CMOS sensor. This was used to collect nadiral footage with the camera's y-axis orthogonal to the direction of flow. Video was collected by the UAS for $4\,\mathrm{min}\ 18\,\mathrm{s}$ whilst hovering ~~in an approximately stationary position~~ at an elevation of approximately $20\,\mathrm{m}$ over the field of interest (Figure 2a). Footage was recorded at a pixel resolution of 1920×1080, and frame rate of $30\,\mathrm{Hz}$. The second approach consisted of a GoPro Hero 4 mounted at an oblique angle on a stationary telescopic pole at a height of approximately $2\,\mathrm{m}$ above the water surface. Video footage was simultaneously collected for $5\,\mathrm{min}\ 37\,\mathrm{s}$ at a pixel resolution of 1920×1080, and frame rate of $30\,\mathrm{Hz}$. During ~~this~~ the period of recording, sequences consisting of both unseeded flow, and artificially seeded flow are visible. For the seeded element, cornstarch ecofoam chips

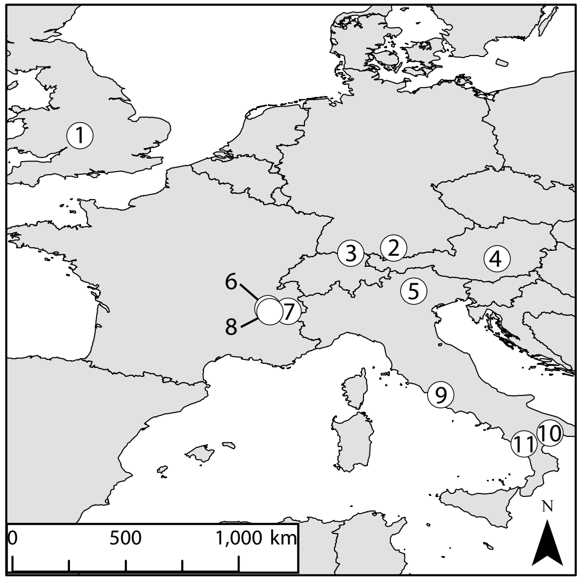

Figure 1. ~~Geographical locations~~ Locations of the monitoring sites from which data is presented. Numbers correspond with the in-text subsections: (~~a~~1) River Arrow, UK; (~~b~~2) River ~~Dart~~Thalhofen, ~~UK~~Germany; (~~c~~3) Murg River~~Thalhofen~~, ~~Germany~~Switzerland; (~~d~~4) ~~Murg~~ Alpine River, ~~Switzerland~~Austria; (~~e~~5) River Brenta, Italy; (~~f~~6) La Morge, France; (~~g~~7) St-Julien torrent, France; (~~h~~8) River La Vence, France; (~~i~~9) River Tiber, Italy; (~~j~~10) River Bradano, Italy; (~~k~~11) River Noce, Italy. Not shown: (12) Castor River~~Karehalla~~, ~~India~~Canada; (13) Salmon River, Canada. Map spatial reference: ETRS (1989).

were added to the water surface immediately upstream of the area of interest. These tracers are clearly visible in the footage and are distributed evenly in the cross-section. Seeding was carried out to enhance the availability of traceable features in the low-flow conditions.

From the recordings, ~~four~~ datasets each consisting of 99 consecutive images (sampled at a frame rate of 5 Hz, and converted to grayscale intensity) were extracted from both the UAS and GoPro footage under both seeded and unseeded conditions. As a result of camera movement for both the UAS and GoPro footage, image sequence stabilisation was carried out using Fudaa-LSPIV (Table A1). In order to enable the conversion of pixel units to metric units a total of ten ground control points (GCPs), which were visible throughout the duration of the video, were distributed across both banks (Figure 2a). These GCPs were surveyed and their positions utilised for image orthorectification using Fudaa-LSPIV (Table A1). Subsequently, the orthorectified images have a scaling of $0.0174\,\mathrm{m\,px^{-1}}$ (Figure 2b). ~~Validation~~

Reference data was obtained ~~for five cross-sections, spaced approximately 1.5–2 m apart through the use~~ through the deployment of a Valeport 801 electromagnetic current meter. ~~This velocity data was obtained~~ Measurements were made for a period of 30 s just below the water surface ~~.~~ with the time-averaged value being reported. Measurements were obtained for five cross-sections spaced approximately -2 m apart, within which, 9–10 individual measurements were obtained with a spacing of 0.5 m between

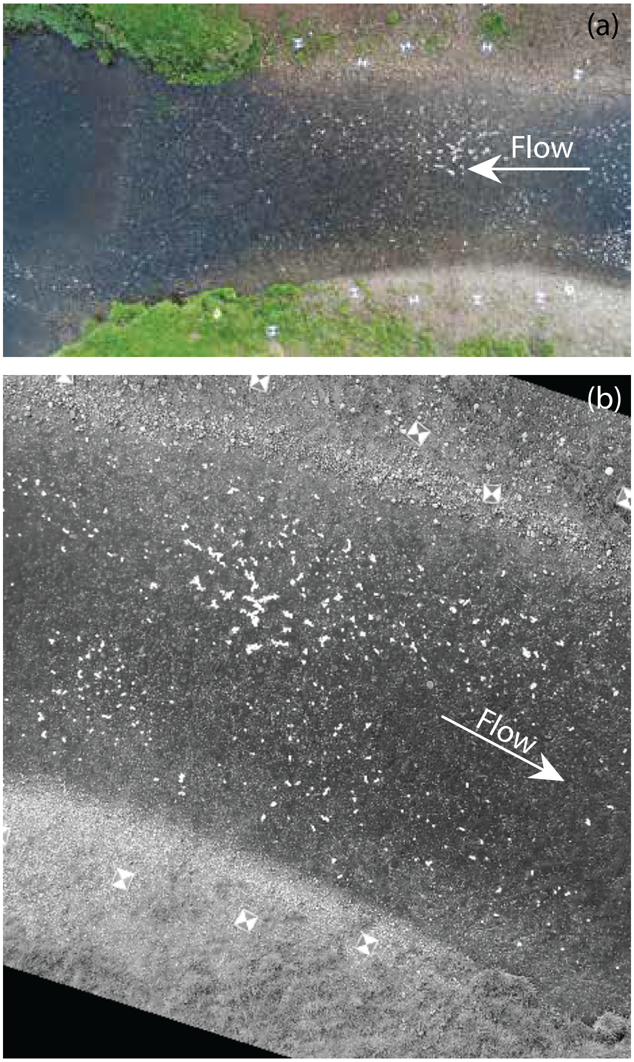

~~(a) Footage acquired by the Phantom 4 UAS over the River Arrow, and (b) following orthorectification and grayscale conversion. The Ecofoam chips and ground control points are clearly visible in both images.~~

Figure 2. (a) Footage acquired by the Phantom 4 UAS over the River Arrow, and (b) following orthorectification and grayscale conversion. The Ecofoam chips and ground control points are clearly visible in both images. The direction of flow is indicated by the arrows.

each. The location of each measurement is provided in pixel units based on the stabilised and orthorectified imagery of the UAS and GoPro.

2.2 ~~River Dart, UK~~

~~In the UK, a dense network of hydrometric monitoring stations is in place for both water resources and flood prediction purposes. However, under the most challenging conditions, current operational approaches for monitoring river flow may~~

~~be sub-optimal. The first of a series of image-based monitoring solutions was installed on the River Dart in collaboration with the Environment Agency. This is a rapidly responding $248\,\mathrm{km}^2$ catchment draining the uplands of Dartmoor, with a channel width of $25\,\mathrm{m}$ under normal flow conditions. Here, a Hikvision DS-2CD2T42WD-I8 $6\,\mathrm{mm}$ IP camera was mounted at an oblique angle (77from nadir), and connected to a Raspberry Pi 3 Model B. This system was configured to record and transmit videos at a resolution of 1920×1080px and a frame rate of $19\,\mathrm{Hz}$ to online servers (AWS S3). The system was commissioned in March 2018 and has since been collecting and transmitting $10\,\mathrm{s}$ videos at $15\,\mathrm{min}$ intervals. No artificial tracers are introduced to the fluvial environment to aid tracking, rather the presence of naturally occurring features are used in the analysis of surface velocities. Following collection, images underwent correction for lens distortion, and have been orthorectified using KLT-IV (Table A1). This results in images where each pixel has a spatial scale of $0.02\,\mathrm{m}$. Here we present five sequences of orthorectified images collected across a range of flows spanning approximately three orders of magnitude (10^0 - $10^2\,\mathrm{m}^3\,\mathrm{s}^{-1}$) at the original frame rate. To supplement this footage, validation data is available in the form of acoustic Doppler current profiler transects conducted at the same river stage as the video footage was collected ($\pm\,0.01\,\mathrm{m}$).~~

2.2 River Thalhofen, Germany

On 27th July 2017, a Vivotek IB836BA-HT network surveillance camera was utilised to capture footage for image velocimetry analysis on the River Thalhofen in Germany. At the time of deployment, the river width was approximately $28\,\mathrm{m}$, the river stage was $1.45\,\mathrm{m}$, and ADCP derived discharge ~~was $52.515\,\mathrm{m}^3\,\mathrm{s}^{-1}$~~ and mean velocity were $52.515\,\mathrm{m}^3\,\mathrm{s}^{-1}$ and $1.7\,\mathrm{m\,s}^{-1}$ respectively. The camera was fixed in location with the camera lens at an approximate angle of 25° from nadir and the image y-axis approximately 5° from being perpendicular to the direction of flow. Images were collected for a duration of $2\,\mathrm{s}$ at a resolution of ~~1280×800~~1280×800px and frame rate of $30\,\mathrm{Hz}$. Despite the presence of highly turbid water, which can diminish contrast across the water surface, the presence of highly visible turbulent structures advecting downstream ~~offer~~ offers the potential for the extraction of surface velocity information from these images. Image pre-processing consisted of orthorectification (using Photrack software (Table 1A)), and color conversion to gray-scale. 56 consecutive images which have been subjected to these processing steps are presented here at their original frame rate of $30\,\mathrm{Hz}$. The pixel dimensions of the processed imagery are $0.01\,\mathrm{m}$ in the x and y-axis. ~~Validation~~

Reference data was acquired by means of a Teledyne RiverPro ADCP ~~.~~ and consists of a single transect consisting of 280 measurements along the cross-section with an average spacing of $0.09\,\mathrm{m}$. ADCP data was acquired with a bin-depth of $0.06\,\mathrm{m}$ with the upper-most measurement occurring at a distance of $0.22\,\mathrm{m}$ below the water surface.

2.3 Murg River, Switzerland

On the ~~4~~6th April 2016, aerial surveys were undertaken in order to acquire imagery for determining the bathymetry, surface velocity, and to subsequently derive the flow discharge of the Murg River, Switzerland (Detert et al., 2017). The experiment took place in the middle reaches of the catchment, with a contributing area of $212\,\mathrm{km}^2$. The experimental reach was a stable, straight section totalling $75\,\mathrm{m}$ in length, along which, the water depth was approximately $0.35\,\mathrm{m}$ and channel width was $12\,\mathrm{m}$. The discharge at the time of survey was . For the aerial survey a DJI Phantom FC40 was deployed at a stable altitude of $30\,\mathrm{m}$

to track the movement of artificial tracers throughout the reach. The UAS was equipped with a GoPro Hero3+ black edition 4K camera, capable of capturing a large spatial footprint whilst deployed at a relatively low altitude. However, this also generates a considerable barrel distortion effect which must be overcome during image processing. This system was used to collect nadiral footage with the camera's y-axis perpendicular to the flow direction. Video footage was acquired for a period of $2\,\mathrm{min}\ 11\,\mathrm{s}$ at a pixel resolution of ~~4096×2160~~ 4096×2160 and a frame rate of $12\,\mathrm{Hz}$. During image acquisition, the water was clear, with the channel bed visible in places. These conditions resulted in a lack of naturally occurring features visible on the water surface that could be used to determine surface velocity. Therefore, throughout the duration of the experiment, spruce wood chips were applied to the water surface from a bridge at the upper extent of the monitored reach. This artificial seeding produced a dense, vivid, and homogeneously distributed pattern of features, the displacement rate of which is considered to equate to the surface velocity. From the video recordings, 1000 images were orthorectified using Photoscan (Agisoft). This was achieved through the input of geographical coordinates relating to 14 GCPs that were visible at varying times throughout image sequence. This approach is discussed further in Detert et al. (2017). The subsequent orthorectified images are presented at a time-step of $0.083\,\mathrm{s}$ and the raster pixel scale was consistently set at 64px m^{-1}, equivalent to pixel dimensions of $0.0156\,\mathrm{m}$ in the x-axis and y-axis. Meta-data describing the scale of the image per pixel, as well as the [x,y] coordinate of the upper left pixel of each image are provided in the corresponding .jgw file. ~~Validation~~

Reference data was acquired through the deployment of a Teledyne RDI StreamPro ADCP across a single transect in the upper reaches of the studied site. ADCP data was acquired with a bin-depth of $0.02\,\mathrm{m}$ with the upper-most measurement occurring at a distance of $0.14\,\mathrm{m}$ below the water surface. A total of 85 measurements of the velocity magnitude are presented with an average spacing of $0.14\,\mathrm{m}$.

2.4 Alpine River, Austria

On the 7th August 2019, aerial surveys were undertaken in order to assess the flow conditions at the turbine outlet of a hydropower dam, the entrance of a fish passage, and the area immediately downstream of these features (Strelnikova et al., 2020). The Alpine river (epithet), is located in Austria, and can be characterised as having a nivo-glacial hydrological regime, with a drainage area of $1057\,\mathrm{km}^2$ and a mean flow discharge of over $32\,\mathrm{m}^3\,\mathrm{s}^{-1}$. At the time of data acquisition the water turbidity was minimal, such that a rocky brown-green riverbed was distinctly visible. Several rocky islands and multiple boulders were located in the middle of the river section of interest. The river section contained turbulent spots and was characterised by heterogeneous flow conditions, with partially opposite flow directions and velocities ranging from 0 to approximately $2\,\mathrm{m\,s}^{-1}$. Within the study area, the river was up to $35\,\mathrm{m}$ wide, with depths ranging from 0.10 to $2\,\mathrm{m}$.

Footage of the area was recorded using a DJI Mavic Pro UAS in a hovering mode from an altitude of $50\,\mathrm{m}$ at a frame rate of $25\,\mathrm{Hz}$, with a resolution of 3840×2160 px. The built-in camera of the UAS was directed at nadir. During data acquisition, the flow was artificially seeded with biodegradable cornstarch ecofoam. Individual ecofoam pieces had cylindrical shape, $1.5{-}2\,\mathrm{cm}$ in diameter and $4.5{-}6\,\mathrm{cm}$ in length. Tracers were added into the flow from seven locations: over the entrance into the fish ladder, over the turbine outlet, from islands and from both banks. The duration of an acquired video was $5\,\mathrm{min}$. From

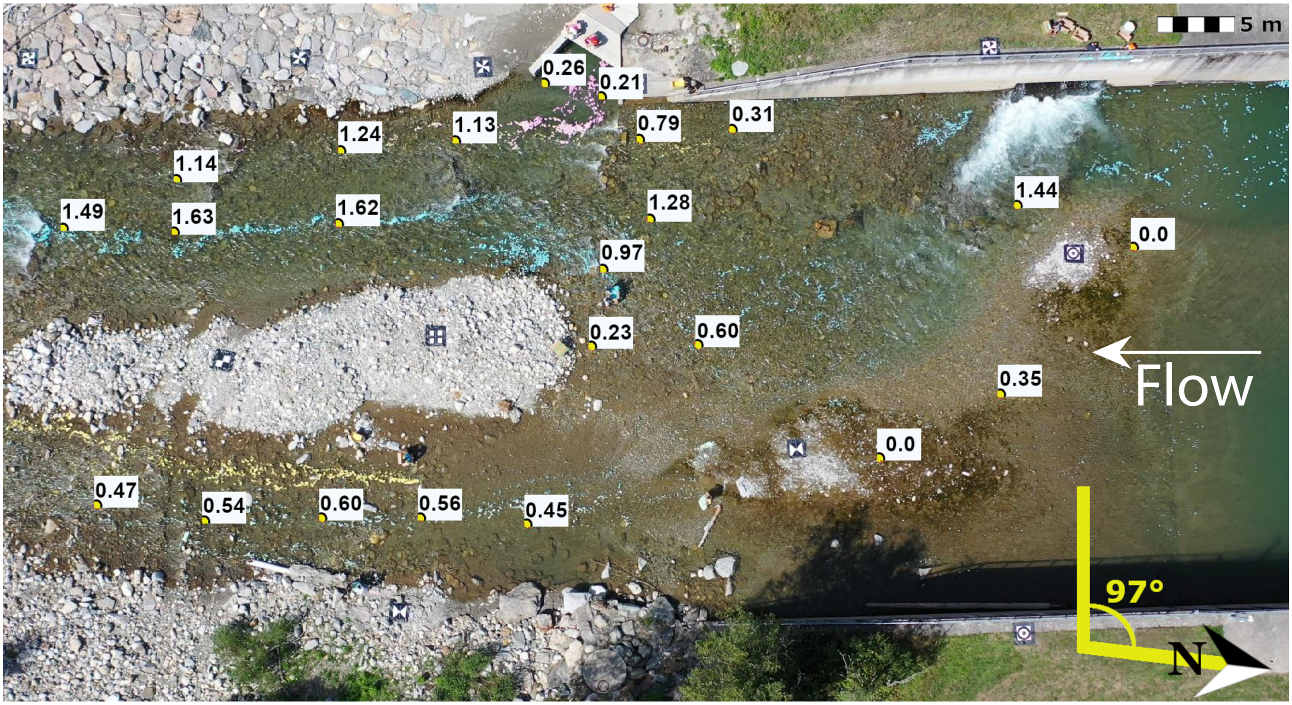

Figure 3. A snapshot from the footage collected near a fish ladder and distribution of reference measurements with corresponding velocity magnitudes ($\mathrm{m\,s^{-1}}$). The dominant direction of flow is indicated by the arrow.

this video, a dataset of 897 images was extracted at 12.5 Hz and stabilised using a custom MATLAB script. A subset of the footage was used in a study described by Strelnikova et al. (2020).

For image calibration, eleven GCPs visible in each of the extracted frames were used. Seven GCPs were distributed across both river banks, and four GCPs were located on the islands. The GCPs were surveyed with the use of a differential GPS with an accuracy of ± 3 cm. The pixel dimensions of the calibrated imagery are $0.021\ \mathrm{m}$ in the x and y-axis.

An OTT C31 propeller current meter was used to perform reference measurement just below the water surface at 23 locations. During reference data acquisition the propeller axis aligned with the direction of the flow. The duration of measurement at each point was $1\ \mathrm{min}$. The distribution of reference measurements (Figure 3) was selected in a way that described all important components of the heterogeneous flow: the flow from the fish ladder entrance, the dominant flow from the turbine outlet, areas around the main flow curve, and two branches of the main flow after its split. Flow directions were determined using a compass with $10°$ precision in degrees from north. The footage was recorded in a way that north corresponded to $97°$ measured in the clockwise direction from the image top (see the north arrow in the bottom right corner of Figure 3). The locations of reference measurements were determined with the use of a differential GPS with an accuracy of ± 3 cm. The accuracy of the propeller current meter was $\pm 2\%$.

2.5 River Brenta, Italy

Two distinct experimental approaches have been adopted to generate datasets that describe flows in the $252\,\mathrm{km}^2$ catchment of the River Brenta. The first involved the temporary installation of a GoPro Hero 4 Black Edition camera attached to a telescopic apparatus on the downstream side of a bridge (Tauro et al., 2014). During this deployment, river flow was low with ~~a~~ an observed mean velocity of $0.38\,\mathrm{m\,s^{-1}}$. To compensate for the lack of naturally ~~visible tracers~~ occurring features on the water ~~'s surface. To compensate for this~~surface, wood-chips were manually added to the river upstream of the monitoring site resulting in continuous, and relatively homogeneous coverage for the $20\,\mathrm{seconds}$ duration of the image sequences. The camera's field of view was ~~9.5×~~$9.5 \times 5.3\,\mathrm{m}^2$ and it was configured to collect ~~1920×1080~~ 1920×1080 HD videos at a frame rate of $50\,\mathrm{Hz}$. Distortion of the images as a result of the fish-eye lens was removed using the open-source software *GoPro Studio*. No subsequent orthorectification of the images was required due to the camera apparatus being installed perpendicular to the water surface. The pixel dimensions of the processed imagery were $0.005\,\mathrm{m}$ in the x-axis and y-axis. This could be established either through the projection of two lasers at a fixed and known distance apart to the surface of the river or through identification of a fixed and known object in the field of view. In terms of pre-processing of the imagery, an area of ~~552×375~~ 552×375 pixels in the bottom right corner of the images was masked with a black patch. This was to eliminate noise generated by mobile vegetation within the frame. Original RGB images were converted to gray-scale intensity by eliminating hue and saturation information and retaining the luminance. To emphasize lighter particles against a dark background, images were gamma corrected to darken mid-tones. A total of twelve separate image sequences lasting ~~twenty seconds, subsampled~~ $20\,\mathrm{s}$, sub-sampled at $25\,\mathrm{Hz}$, and consisting of 500 frames each are presented here.

The second experimental approach involved the temporary deployment of a FLIR Systems AB ThermaCAM SC500. This was suspended from a mobile supporting structure on the downstream side of a bridge at approximately $7\,\mathrm{m}$ above the water surface (Tauro and Grimaldi, 2017). As opposed to capturing images in the usual red, green, and blue bands, this camera is sensitive to thermal infrared radiation, generating a monochrome image with values proportionate to the thermal properties of the objects within the field of view. The application of this approach for image velocimetry requires a distinct thermal signal to be present from either natural (e.g. tributary confluences with water of differing thermal properties), or artificial sources. In this instance, an artificial thermal signal was introduced in the form of ice dices. These were deployed upstream of the bridge and were observed transiting across the field of view as a result of their thermal properties being sufficiently different to that of the water surface. Despite the image resolution being a modest ~~318 ×197~~ 318×197 pixels with a frame rate of ~~5Hz~~$5\,\mathrm{Hz}$, this was still sufficient to enable movement of the ice-dices to be tracked. Geometric calibration of the images was achieved by identifying features of known dimensions within the video sequence (i.e. three wooden sticks). The pixel dimensions of the processed imagery are ~~0.009m~~$0.009\,\mathrm{m}$ in the x- and y-axis. Here we present an image sequence consisting of 80 consecutive frames captured over ~~sixteen seconds. Validation~~ $16\,\mathrm{s}$.

Reference validation data is available in the form of velocity measurements taken at just ~~3cm~~ $3\,\mathrm{cm}$ below the water surface at four locations along the stream cross-section using an OTT Hydromet C2 current meter. At each measurement location 12 replicate measurements were made (Tauro et al., 2017).

2.6 La Morge River, France

~~As part of~~ Within Electricité De France's (EDF) network of over 300 hydrological monitoring stations for the optimal management of water resources, image-based velocimetry approaches have ~~been deployed to supplement their existing network of over 300 hydrological monitoring stations~~recently been adopted. This approach has been specifically adopted with the aim of reducing uncertainty under high flow conditions (Hauet, 2016). These conditions can develop rapidly, particularly during the summer months as a result of convective storms, posing difficulties for traditional monitoring approaches. However, this setup may also be applied to capture images for the determination of surface velocity under more quiescent conditions. Here, we present images captured on 13th January 2015 in the small ($46\,\mathrm{km}^2$), urban catchment of La Morge with a mean altitude of $270\,\mathrm{m}$. Flow conditions were typical with a cross-section width of $7.2\,\mathrm{m}$, mean depth of $0.41\,\mathrm{m}$, and mean velocity of 0.39 $\mathrm{m\,s^{-1}}$. The imaging system used consisted of an analog Panasonic WV-CP500 camera with a focal length of $4\,\mathrm{mm}$. This camera was mounted at an elevated position on a $3\,\mathrm{m}$ pole on the right bank of the channel, oriented in an upstream direction. Images were collected with an effective pixel resolution of 640×480 at a frame rate of $5\,\mathrm{Hz}$ for a duration of $10\,\mathrm{s}$, resulting in the generation of 48 images. On this occasion, manual seeding of corn chips took place immediately upstream of the camera's field-of-view to enhance the occurrence of features for tracking purposes. This is typically required where natural seeding is inhomogeneous, or completely lacking~~, in some settings under low-flow conditions~~. Following acquisition of the footage, images were converted to grayscale, and orthorectified using Fudaa-LSPIV to generate images in which 1 pixel represents a real-world distance of $0.01\,\mathrm{m}$. ~~Validation velocity~~

Reference data was acquired $5\,\mathrm{m}$ downstream of the video acquisition location so as to not interfere with the recorded footage. Therefore, comparisons between measured velocities using image velocimetry and traditional gauging methods in the same cross-section is not possible. However, a comparison of the computed river discharge from the differing methods is possible. At the upstream location (the camera monitored reach), water depth measurements are available for two transects separated by approximately $6\,\mathrm{m}$ with an average spacing between points of $0.25\,\mathrm{m}$. Through the application of image velocimetry techniques, water depth measurements, and an appropriate value relating the surface velocity to the depth-averaged velocity (estimated to be 0.85), river discharge can be computed. $5\,\mathrm{m}$ downstream of the camera, velocity data was acquired through the use of a mechanical current meter, with measurements taken at 0.2, 0.6, and 0.8 of the river depth. 15 measurements were made along the cross-section, at intervals of $0.5\,\mathrm{m}$. Detailed measurements are provided along with the river discharge computed from these observations. Given the small distance of $5\,\mathrm{m}$ between the location of the recorded video footage and in-stream measurements, and the lack of gains or losses within the reach, river discharge would be the same value at both locations.

2.7 St-Julien torrent, France

A high-magnitude flash flood ~~event~~ occurred in the St-Julien torrent system during August 2011. This was captured by a local storm chaser using a Canon EOS 5D mark II camera with a $16\,\mathrm{mm}$ fisheye Zenitar lens. Like many headwater systems across Europe, no hydrological monitoring networks are present in this torrent system. Therefore this footage provides a rare insight into the hydraulic processes occurring during a flash flood in a steep, small ($20\,\mathrm{km}^2$), torrent system where mean flow velocities are approximately $6\,\mathrm{m\,s^{-1}}$. The footage itself was recorded at a resolution of ~~1920×1080~~1920×1080px at a frame rate of $25\,\mathrm{Hz}$ (Figure ~~3a~~4a). The footage was not filmed from a fixed location therefore complications involving camera movement, and orthorectification had to be overcome. These steps are explained in detail in Le Boursicaud et al. (2016). Following correction for these factors, a sequence of 51 consecutive and geometrically stable images are produced (Figure ~~3b~~4b). Each pixel width represents a metric scale of $0.03\,\mathrm{m}$. Despite the lack of detailed reference velocity measurements for this case study, researchers interested in reconstructing flash flood processes may find it valuable to understand how the range of available methods perform relative to each other given that image velocimetry techniques perhaps offer the best opportunity to estimate flows under these extreme conditions.

2.8 River La Vence, France

On May 8th, 2019, a Samsung Galaxy S7 was utilised to capture footage for image velocimetry analysis on the River La Vence, a $63.75\,\mathrm{km}^2$ catchment in France. At the time of deployment, the river width was approximately ~~$6.7\,\mathrm{m}$, the river stage was $0.44\,\mathrm{m}$, with an observed~~ $6.3\,\mathrm{m}$, with a river stage of $0.44\,\mathrm{m}$. A discharge of $1.15\,\mathrm{m^3\,s^{-1}}$, and mean velocity of $0.65\,\mathrm{m\,s^{-1}}$ were observed. The camera was fixed in location with the camera lens ~~at an approximately 31° from the water surface~~ angled at approximately 31° from nadir and the image x-axis at approximately perpendicular to the direction of flow. Images were collected for a duration of ~~5 seconds~~ $5\,\mathrm{s}$ at a resolution of ~~1920×1080~~1920×1080px and frame rate of ~~30Hz~~$30\,\mathrm{Hz}$. The presence of visible turbulent structures advecting downstream offer the potential for the extraction of surface velocity information from this footage. Image pre-processing consisted of orthorectification, and color conversion to gray-scale. 150 consecutive images which have been subjected to these processing steps are presented here at their original frame rate of ~~30Hz~~$30\,\mathrm{Hz}$. The pixel dimensions of the processed imagery are ~~0.008m~~ $0.008\,\mathrm{m}$ in the x and y-axis. ~~Validation data was recorded~~

Reference data was acquired by means of a ~~mobile ADCP (~~HydroProfiler M-pro ~~).~~ ADCP and consists of a single transect consisting of 8 measurements with an average spacing of $0.7\,\mathrm{m}$. ADCP data was acquired with a bin-depth of $0.003\,\mathrm{m}$ with the upper-most measurement occurring at a distance of $0.101\,\mathrm{m}$ below the water surface.

2.9 River Tiber, Italy

A permanent gauge station on the River Tiber, Italy was installed to test the feasibility for automated image velocimetry methods to quantify the flow rates of a major European river with a catchment area of $17\,460\,\mathrm{km}^2$. This deployment involves the use of a Mobotix FlexMount S15 IP camera attached to the underside of Ponte del Foro Italico, in the city of Rome (Tauro et al., 2016a). The wide angle lens on the SP15 camera introduces distortion into the images, which was subsequently removed using the Adobe Photoshop Lens correction filter. In a similar setup to the first of the River Brenta approaches, this camera is positioned orthogonal to the water surface, thereby circumventing the need for orthorectification of the generated images. Transformation of the camera pixels (px) to metric units (~~m~~m) was again achieved by firing lasers of a known distance apart at the water surface. The image can be scaled to metric distances given: ~~1px~~ 1px = $0.016\,\mathrm{m}$. The camera itself generated

Figure 4. (a) Original footage of a flash flood in the St-Julien torrent acquired by a storm chaser equipped with Canon EOS 5D mark II camera~~. The direction of flow is from the top of the frame, moving towards the bottom of the image~~; (b) Orthorectified and geometrically stable image with the field of view clipped to the lower 50% of the image. The direction of flow is ~~from~~ indicated by the ~~bottom of the frame, moving towards the top of the image~~arrows.

videos with a resolution of ~~2048×768~~2048 × 768px. However these were sub-sampled to ~~865×530~~865 × 530px at a frame rate of $\approx 6.95\,\mathrm{Hz}$ during pre-possessing. The data specifically presented here consists of 410 consecutive frames collected over a 60 second period during a moderate flood event in February 2015. At the time of acquisition, the river stage was $7.23\,\mathrm{m}$, and average surface velocity (measured by a RVM20 speed surface velocity radar) was $2.33\,\mathrm{m\,s^{-1}}$ (Tauro et al., 2017). Whilst only a single reference velocity value is available, this measurement is representative of the surface velocities within a surrounding area of approximately 3 x $3\,\mathrm{m}^2$. The approximate spatial footprint of the surface velocity radar measurement is provided in pixel units.

2.10 River Bradano, Italy

On 14th October 2016, an experiment was undertaken in order to explore the optimal setup for the acquisition of surface flow velocity measurements using an UAS (Dal Sasso et al., 2018). The experiment took place in the valley portion of the Bradano River, located in the Basilicata region of Italy. This large alluvial river has a catchment area of $2581\,\mathrm{km}^2$ and is characterised by low gradient (0.1%) and low relative submergence (Dal Sasso et al., 2018). At the time of the experiment, the cross-section width was $11.4\,\mathrm{m}$, with a maximum depth of $0.80\,\mathrm{m}$. The average surface velocity was $0.75\,\mathrm{m\,s^{-1}}$ and total discharge was $3.97\,\mathrm{m^3\,s^{-1}}$. During the experiment, a DJI Phantom 3 Pro UAS equipped with a Sony EXMOR 1/2.3” CMOS camera sensor was deployed.

~~This system~~ The UAS hovered over the centre of the River Bradano with a nadir camera positioned perpendicular to the direction of flow. ~~Flight altitude was set at 10 m in order to capture an~~ An area of $17.0 \times 9.6\mathrm{m}^2$ was imaged, including the entire cross-section of interest (with a width of approximately $11.4\,\mathrm{m}$). Video footage was captured for a duration of $1\,\mathrm{min}\ 43\,\mathrm{s}$ at a pixel resolution of 1920×1080, and a frame rate of $24\,\mathrm{Hz}$. Due to the high turbidity of the flow, there is a weak natural contrast across the image which diminishes the number of naturally occurring, visible tracers. Therefore, throughout the duration of the footage, operatives manually introduced charcoal to the water surface immediately upstream of the monitoring site. The color of these particles was sufficiently distinct from the background to enable their displacement to be optically tracked. However, the distribution of these tracers is generally limited to the central portion of the flow which may limit the availability of traceable features towards the channel boundaries. Following collection of the footage, a number of processing steps were subsequently undertaken. This included conversion of the grayscale images to black and white, and contrast correction in order to more prominently highlight the artificial tracers on the water surface. 600 images which have been subjected to these processing steps are available at their original resolution and frame rate. An addition processing step involved the stabilisation of the image sequence to minimise apparent movement of the platform. Transformation of the ~~camera~~ images from pixel units to metric distance can be achieved using the following function: $1\mathrm{px} = 0.009\,\mathrm{m}$. Validation data in the form of surface velocities ~~were obtained at five~~ was obtained at seven points in the cross-section, at $1\,\mathrm{m}$ intervals using a Seba F1 current flow meter. The locations of these measurements are provided in pixels relative to the first frame of the stabilised image sequence.

2.11 River Noce, Italy

On 26th July 2017, in the middle reaches of the 413 km^2, single-thread, River Noce, a DJI Phantom 3 Pro UAS Sony EXMOR 1/2.3” CMOS sensor was deployed to capture footage for image velocimetry analysis (Dal Sasso et al., 2018). At the time of deployment, water levels were low with an observed discharge of $1.70\,\mathrm{m^3\,s^{-1}}$ and mean velocity of $0.43\,\mathrm{m\,s^{-1}}$. Turbidity was also minimal resulting in the gravel bed being distinctly visible in the footage. The camera was oriented with its x-axis perpendicular to the water surface enabling the 14.6 m wide channel to be fully observed (Figure ~~4a~~5a). Images were collected for a duration of 1 min 48 s at a resolution of ~~3840×2160~~3840×2160px and frame rate of 24 Hz. The clear water and bright sunlight results in non-homogeneous illumination of the water surface. This is particularly apparent in the lower left quarter of the video frame. Naturally occurring tracers are also largely absent making these challenging conditions for the application of image velocimetry techniques. To offset these issues, wood chips were introduced upstream of the monitoring location. These features were visibly brighter than the background enabling their transition to be detected optically. Image processing consisted of contrast stretching and conversion of grayscale images to black and white in order to enhance the visibility of the artificial tracers against the background (Figure ~~4b~~5b). 70 consecutive images which have been subjected to these processing steps are presented here at a downscaled resolution of ~~1920×1080~~1920×1080px and frame rate of 12 Hz. Following sub-sampling, each pixel in the image represents a distance of 0.009 m in metric units. Validation data in the form of surface velocities were obtained at ~~ten~~ thirteen locations, at 1 m intervals, along the cross-section using a Seba F1 current flow meter. The locations for each of these measurements is provided in pixel units.

2.12 Castor River~~Karehalla~~, ~~India~~Canada

~~On 19th June 2018, a Vivotek IB836BA-HT network surveillance camera was utilised to capture footage for image velocimetry analysis on the River Karehalla in India (12.835N, 75.716E~~ Here we present footage acquired from the middle reaches of the Castor River in Ontario, Canada (45.26194° Latitude, -75.34444° Longitude). At ~~the time of deployment~~this location, the channel ~~width was approximately 8.36 m, the river stage was 0.606 m, with an observed discharge of 3.003 $\mathrm{m^3\,s^{-1}}$. The camera was fixed in location with the camera lens at an approximately 30from nadir~~is a stable, single thread, meandering river with a catchment contributing area of 439 km^2. Footage was acquired on two separate occasions, consisting of very different flow conditions:

The first set of videos were acquired on 10th April 2019 using a Hikvision DS-2CD2T42WD-I5 4mm IP camera. This was mounted on the left bank at an oblique angle of 57° from nadir. Video footage was captured consisting of three, 30 second videos at a resolution of 2688×1520px and frame rate of 20 Hz. The first $2-3$ s of each recording have been removed from the submission as these frames experienced compression and frame rate issues. However, the remainder of the video is unaffected. The videos were captured over a duration of approximately 4.5 h and over this time the river stage was stable, varying between 3.772 m at 11:25, 3.769 m at 13:45, and 3.77 m at 15:55 (local time). Under these moderate flow conditions, mean velocity was observed to be $1.26\,\mathrm{m\,s^{-1}}$, with mean and maximum depths of 0.80 and 1.19 m respectively within the 27 m wide river. No image stabilisation was performed on the image sequence and the imagery was orthorectified using KLT-IV and the use

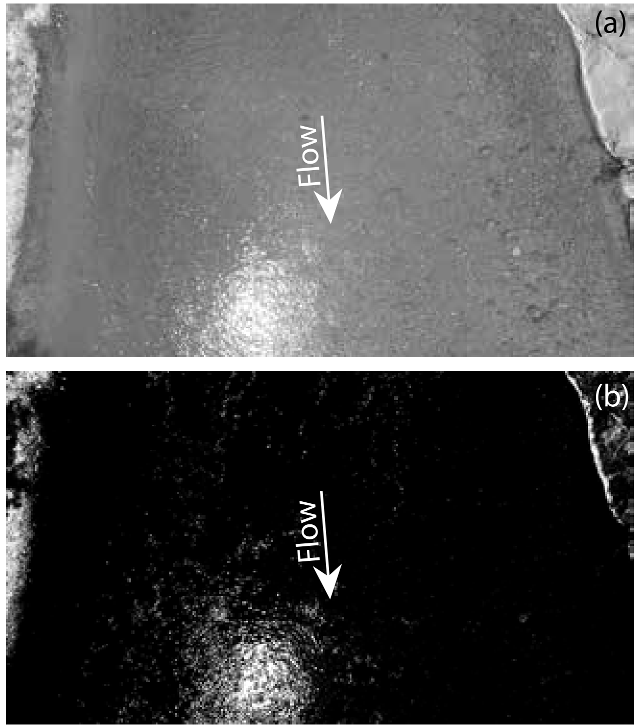

Figure 5. (a) Grayscale footage acquired by the Phantom 3 UAS over the River Noce, and (b) following contrast stretching. The direction of flow is indicated by the arrows.

of twelve ground control points. These control points were placed at varying heights across both sides of the channel, and the distances, horizontal and vertical angles between points were surveyed using a tripod mounted Leica S910. This enabled a local coordinate system to developed relative to a local benchmark. In the resultant imagery each image pixel represents a distance of $0.01\,\mathrm{m}$ in metric units.

Reference data was acquired through the deployment of a Teledyne RDI StreamPro ADCP with four transects being completed across a single cross-section. ADCP data was acquired with a bin-depth of $0.05\,\mathrm{m}$ with the upper-most measurement occurring at a distance of $0.17\,\mathrm{m}$ below the water surface. Between 149 and ~~the image x-axis at approximately 5from perpendicular to the direction of flow. Images were collected for a duration of 4.6 s~~ 219 velocity magnitude measurements are reported for each transect with an average spacing between measurements of - $0.18\,\mathrm{m}$. The location of each velocity magnitude measurement is reported in pixel units based on the orthorectified imagery.

The second video set obtained at Castor River was acquired on 9th July 2019 and consists of a single, 27 s video. This was acquired from the left bank using a ACTI A31 IP camera, mounted at an oblique angle of 54° from nadir. Video footage was recorded at a resolution of ~~1920×1080~~1920×1080px and frame rate of 30 Hz. ~~Highly visible, naturally occurring, turbulent structures that are advecting downstream offer the potential for the extraction of surface velocity information from these images. Image pre-processing consisted of orthorectification, and color conversion to gray-scale. 144 consecutive images which have~~

~~been subjected to these processing steps are presented here at their original~~ At the time of acquisition, river levels were low, with a reported stage of 3.128 m. At this time, the river was 21 m wide with a mean and maximum depth of 0.45 and 0.62 m respectively. Observed discharge was $0.926\,\mathrm{m^3\,s^{-1}}$ with a mean velocity of $0.13\,\mathrm{m\,s^{-1}}$. No image stabilisation was performed on the image sequence and the imagery was orthorectified using KLT-IV and the same ground control points as the previous set of videos. In the resultant imagery each image pixel represents a distance of 0.01 m in metric units. Reference data was acquired using a FlowTracker2 handheld acoustic Doppler velocimeter. Velocity measurements were made at four locations along a single cross-section and at percentage depths of 0 (i.e. water surface), 20, 40, 60, 80, and 100%. The x and y velocity components are reported along with the mean velocity. The location of each velocity measurement is reported in pixel units based on the orthorectified imagery.

2.13 Salmon River, Canada

On the 4th June 2019, a DJI Phantom 4 Pro was used to acquire footage over the Salmon River in British Columbia, Canada (50.312222° Latitude, -125.907500° Longitude). Footage was acquired immediately downstream of the confluence between the Salmon River and the smaller White River. Here, the catchment contributing area is $1210\,\mathrm{km^2}$, and a 59 m wide, single thread channel is present. At the time of image acquisition, river levels were low, with an average depth of 0.65 m, a reported discharge of $22.9\,\mathrm{m^3\,s^{-1}}$, and mean velocity of $0.65\,\mathrm{m\,s^{-1}}$. A 1 min video was collected with a view angle of approximately nadir whilst hovering at an elevation of 102 m over the field of interest. The footage was acquired at a resolution of 1920×1080px and a frame rate of ~~30 Hz. The pixel dimensions of the processed imagery is 0.01 m in the x and y-axis. Validation~~ 24 Hz. Present within the field of view are four ground control points, located on both sides of the channel. The straight-line distances between each of the ground control points were measured and a local coordinate system developed following the principles of trilateration. A two-stage processing method was adopted to generate imagery suitable for velocimetry analysis. This consisted of: (i) image stabilisation; and (ii) orthorectification. These were performed using the built-in functionality of KLT-IV (Table A1). Following processing, each image pixel represents a distance of 0.01 m in metric units. Reference velocity data was acquired ~~by means of a HydroProfiler M-pro ADCP.~~ using a FlowTracker handheld acoustic Doppler velocimeter and this consists of measurements at twenty six locations along a single cross-section at intervals of approximately 3 m. These measurements were obtained at 60% of the water depth and the mean velocity is reported. The location of each velocity measurement is reported in pixel units based on the orthorectified imagery.

3 Conclusions

Applied hydrology research, ~~focussing~~ focusing on the quantification of fluid flow processes in river systems, has been greatly enhanced by the availability of large-scale image velocimetry techniques (e.g. Table A1). The flexibility of these approaches has led to improvements in the understanding of hydrological processes in otherwise difficult to access environments. This has been possible through image capture using a range of platforms including: unmanned aerial systems, thermal infra-red cameras, Go-Pro's, and IP cameras, which enable non-contact sensing of the waterbody. Consequently, a growing, but disparate, range of imagery datasets have been produced (e.g. Table A2). Here we collate and describe a range of these example datasets, most of which have validation data in the form of velocity measurements undertaken using standard operational approaches (e.g. current flow meter, ADCP, radar). This unique dataset offers the hydrological community the opportunity to conduct image velocimetry benchmarking studies in order to assess the accuracy of existing approaches under a range of differing conditions. The generation of similar standardised sets of images are widely used to evaluate the effectiveness and accuracy of algorithms in related fields such as fluid mechanics (e.g. Okamoto et al., 2000), and we envisage such a dataset for large-scale fluvial environments will encourage further scientific assessment and development of image velocimetry approaches. Ultimately, forensic assessment of these techniques will provide researchers and competent authorities with a greater understanding of their applicability and limitations.

4 Data availability

Datasets presented in this manuscript can be readily downloaded from the following website: ~~. Validation data is available~~ http://doi.org/10.4121/uuid:014d56f7-06dd-49ad-a48c-2282ab10428e. Data includes the footage/imagery required for image velocimetry analysis, plus validation data for 12 of the 13 case studies presented. Please contact the corresponding author ~~for details~~ if further details are required (Perks et al., 2020).

Table A1. Details of software developed for image velocimetry analysis

Software	Key Functions	Availability
Fudaa-LSPIV[a]	Sample images from movies, image orthorectification, cross-correlation, data filtering, discharge computation	Open source interface, free executables
KLT-IV[b]	Lens distortion removal, image stabilisation and orthorectification, tracking individual trajectories, discharge computation	Proprietary software
KU-STIV[c]	Distortion removal, orthorectification, image stabilisation, image pattern coherence	Proprietary software
LSPIV app[d]	Camera calibration, image orthorectification, cross-correlation, image pattern coherence	Free app for Android and iOS
MAT PIV[e]	Image coordinate transformation, cross-correlation, post-processing filters	Free toolbox for MATLAB
OTV[f]	Tracking individual trajectories and average surface flow velocity estimation	Proprietary software
Photrack. SSIV[g]	Image orthorectification, cross-correlation, flow surface structure filtering, results filtering, discharge estimation. Stand-alone camera system for continuous measurement (DischargeKeeper), or in a smart-phone application (DischargeApp)	Proprietary software
PIVlab[h]	Image pre-processing, direct cross-correlation, discrete Fourier transform, sub-pixel solutiona, post-processing tools	Free toolbox for MATLAB
PTVlab[i]	Image pre-processing, cross-correlation, relaxation algorithm, dynamic threshold binarization, iterative relaxation, tracking of individual trajectories, post-processing tools	Free toolbox for MATLAB
PTV-Stream[j]	Tracking individual trajectories and average surface flow velocity estimation	Proprietary software
RIVeR[k]	Image extraction from video, image processing (PIVlab or PTVlab), rectification of velocities to real-world units, discharge calculation	Free toolbox for MATLAB

[a]Le Coz et al. (2014); [b]Perks et al. (2016); [c]Fujita et al. (2007); [d]Tsubaki (2018); [e]Sveen and Cowen (2004); [f]Tauro et al. (2018b); [g]Leitão et al. (2018); [h]Thielicke and Stamhuis (2014); [i]Brevis et al. (2011); [j]Tauro et al. (2019); [k]Patalano et al. (2017)

Table A2. Experimental setup during ~~data~~ image acquisition, details of subsequent image pre-processing, availability of validation data and published analysis.

Identifier	Image Acquisition	Pre-processing	Validation Data	Image Velocimetry Software Used	Published Analysis
River Arrow (a)	DJI Phantom Pro 4 UAS	Conversion to grayscale intensity Orthorectification Image sequence sub-sampled	~~Yes~~ Five cross-sections of 9-10 points using a Valeport ECM	Fudaa-LSPIV	N/A
River Arrow (b)	Go Pro Hero 4	~~Conversion to grayscale intensityOrthorectificationImage sequence sub-sampled~~ As above	~~Yes~~ See Arrow (a)	Fudaa-LSPIV	N/A
~~River Dart Hikvision EXIR Distortion removalOrthorectification Yes KLT-IV N/A River~~ River Thalhofen	Vivotek IB836BA-HT	Orthorectification Conversion to grayscale intensity	~~Yes~~ A single RiverPro ADCP transect	Photrack. SSIV	N/A
Murg River	DJI Phantom FC40 UAS with GoPro Hero3+	Orthorectification	~~Yes~~ A single StreamPro ADCP transect	PIVlab	Detert et al. (2017)
Alpine River	DJI Mavic Pro with Hasselblad 1/2.3" CMOS sensor	None	Water surface velocities measured using an OTT C31 at 23 locations across the field of view	PIVlab	Strelnikova et al. (2020)
River Brenta (a)	GoPro Hero 4	Distortion removal Gamma correction	~~Yes~~ Velocity measurements	PIVlab & PTVlab	Tauro et al. (2017)

Table A2. Continued.

Identifier	Image Acquisition	Pre-processing	Validation Data	Image Velocimetry Software Used	Published Analysis
La Morge	WV-CP500	Orthorectification	15 paired velocity and depth measurements performed 5 m downstream of camera, and depth across two transects within camera field of view	Fudaa-LSPIV	Hauet (2016)
St-Julien torrent	Canon EOS 5D	Distortion removal Orthorectification Image stabilisation	~~No~~ N/A	Fudaa-LSPIV	Le Boursicaud et al. (2016)
River La Vence	Samsung Galaxy S7	Orthorectification Conversion to grayscale intensity	~~Yes~~ A single HydroProfiler M-pro ADCP transect	Photrack. SSIV	N/A
River Tiber	Mobotix S15	Distortion removal Conversion to grayscale intensity	~~Yes~~ A single RVM20 SVR measurement	PIVlab & PTVlab	Tauro et al. (2017)
River Bradano	DJI Phantom 3 Pro UAS with Sony 1/2.3" CMOS sensor	Conversion to black and white images Contrast correction	~~Yes~~ Surface velocities at 7 points within a single cross-section using a SEBA F1	PTVlab	Dal Sasso et al. (2018)
River Noce	DJI Phantom 3 Pro UAS with Sony 1/2.3" CMOS sensor	Contrast stretching Conversion to black and white images Image sequence sub-sampled	~~Yes~~ Surface velocities at 13 points within a single cross-section using a SEBA F1	PTVlab	Dal Sasso et al. (2018)
~~River Karehalla~~ Castor River (a)	~~Vivotek IB836BA-HT~~ Hikvision DS-2CD2T42WD-I5 4mm IP camera	~~Orthorectification~~ Conversion to grayscale Orthorectified	Four StreamPro ADCP transects at a single cross-section	KLT-IV	N/A
Castor River (b)	ACTI A31 IP camera	Conversion to grayscale~~intensity~~ Orthorectified	~~Yes~~ Velocity measurements at four points along a single cross-section at six depths using a FlowTracker2 ADV	~~Photrack. SSIV~~ KLT-IV	N/A

Table A2. Continued.

Identifier	Image Acquisition	Pre-processing	Validation Data	Image Velocimetry Software Used	Published Analysis
Salmon River	DJI Phantom 4 Pro	Conversion to grayscale Stabilised Orthorectified	Velocity measurements at 24 points in a single cross-section using a FlowTracker ADV	KLT-IV	N/A

Author contributions. This article and dataset compilation was initially proposed by SM and SG. MP led the production of the manuscript. Each co-author contributed to the writing, and the contribution of datasets.

Competing interests. The authors declare that they have no conflict of interest.

Acknowledgements. This work was funded by the COST Action CA16219 “HARMONIOUS—Harmonization of UAS techniques for agricultural and natural ecosystems monitoring”. ~~MP and BH acknowledge additional funding from NERC grant NE/K008781/1 “Susceptibility of catchments to INTense RAinfall and flooding (SINATRA)”, and the Environment Agency.~~ SG and FT acknowledge support by Ministero degli Affari Esteri project 2015 Italy-USA PGR00175~~and~~, by POR-FESR 2014-2020 n. 737616 INFRASAFE, and by “Departments of Excellence-2018” Program (Dipartimenti di Eccellenza) of the Italian Ministry of Education, University and Research, DIBAF-Department of University of Tuscia, Project “Landscape 4.0 – food, wellbeing and environment”. The contribution of the Murg River dataset was kindly made available by Dr Martin Detert. ADCP measurements for this case study were provided by Urs Vogel (Limnex AG). The Murg River dataset can also be accessed at: https://figshare.com/articles/S1S2S3_Murg_20160406_zip/4680715/1.

References

Adrian, R. J.: Scattering particle characteristics and their effect on pulsed laser measurements of fluid flow: speckle velocimetry vs particle image velocimetry, Appl. Opt., 23, 1690–1691, https://doi.org/10.1364/AO.23.001690, 1984.

Agisoft: Agisoft PhotoScan Professional Edition (version 1.1.6), https://www.agisoft.com.

Brevis, W., Niño, Y., and H. Jirka, G.: Integrating cross-correlation and relaxation algorithms for particle tracking velocimetry, Experiments in Fluids, 50, 135–147, 2011.

Dal Sasso, S. F., Pizarro, A., Samela, C., Mita, L., and Manfreda, S.: Exploring the optimal experimental setup for surface flow velocity measurements using PTV, Environmental Monitoring and Assessment, 190, 460, https://doi.org/10.1007/s10661-018-6848-3, 2018.

Detert, M. and Weitbrecht, V.: A low-cost airborne velocimetry system: proof of concept, Journal of Hydraulic Research, 53, 532–539, https://doi.org/10.1080/00221686.2015.1054322, 2015.

Detert, M., Johnson, E. D., and Weitbrecht, V.: Proof-of-concept for low-cost and noncontact synoptic airborne river flow measurements, International Journal of Remote Sensing, 38, 2780–2807, https://doi.org/10.1080/01431161.2017.1294782, 2017.

Dudderar, T. D. and Simpkins, P. G.: Laser speckle photography in a fluid medium, Nature, 270, http://dx.doi.org/10.1038/270045a0, 1977.

Fujita, I., Muste, M., and Kruger, A.: Large-scale particle image velocimetry for flow analysis in hydraulic engineering applications, Journal of Hydraulic Research, 36, 397–414, https://doi.org/10.1080/00221689809498626, 1998.

Fujita, I., Watanabe, H., and Tsubaki, R.: Development of a non-intrusive and efficient flow monitoring technique: The space-time image velocimetry (STIV), International Journal of River Basin Management, 5, 105–114, https://doi.org/10.1080/15715124.2007.9635310, 2007.

Harpold, A., Mostaghimi, S., Vlachos, P. P., Brannan, K., and Dillaha, T.: Stream discharge measurement using a large-scale particle image velocimetry (LSPIV) prototype, Transactions of the ASABE, 49, 1791–1805, 2006.

Hauet, A.: Monitoring river flood using fixed image-based stations: Experience feedback from 3 rivers in France, in: River Flow 2016: Iowa City, USA, July 11-14, 2016, edited by Constantinescu, G., Garcia, M., and Hanes, D., pp. 541–547, CRC Press, Boca Raton, USA, https://books.google.co.uk/books?id=blOzDAAAQBAJ, 2016.

ISO 24578:2012: Hydrometry — Acoustic Doppler profiler — Method and application for measurement of flow in open channels, Standard, International Organization for Standardization, Geneva, CH, 2012.

Le Boursicaud, R., Pénard, L., Hauet, A., Thollet, F., and Le Coz, J.: Gauging extreme floods on YouTube: application of LSPIV to home movies for the post-event determination of stream discharges, Hydrological Processes, 30, 90–105, https://doi.org/10.1002/hyp.10532, 2016.

Le Coz, J., Jodeau, M., Hauet, A., Marchand, B., and Le Boursicaud, R.: Image-based velocity and discharge measurements in field and laboratory river engineering studies using the free FUDAA-LSPIV software, Proceedings of the International Conference on Fluvial Hydraulics, River Flow 2014, pp. 1961–1967, 2014.

Leitão, J. P., Peña-Haro, S., Lüthi, B., Scheidegger, A., and de Vitry, M. M.: Urban overland runoff velocity measurement with consumer-grade surveillance cameras and surface structure image velocimetry, Journal of Hydrology, 565, 791 – 804, https://doi.org/https://doi.org/10.1016/j.jhydrol.2018.09.001, http://www.sciencedirect.com/science/article/pii/S0022169418306875, 2018.

Mishra, A. K. and Coulibaly, P.: Developments in hydrometric network design: A review, Reviews of Geophysics, 47, https://doi.org/10.1029/2007RG000243, https://agupubs.onlinelibrary.wiley.com/doi/abs/10.1029/2007RG000243, 2009.

Okamoto, K., Nishio, S., Saga, T., and Kobayashi, T.: Standard images for particle-image velocimetry, Measurement Science and Technology, 11, 685–691, https://doi.org/10.1088/0957-0233/11/6/311, https://doi.org/10.1088%2F0957-0233%2F11%2F6%2F311, 2000.

Patalano, A., García, C. M., and Rodríguez, A.: Rectification of Image Velocity Results (RIVeR): A simple and user-friendly toolbox for large scale water surface Particle Image Velocimetry (PIV) and Particle Tracking Velocimetry (PTV), Computers & Geosciences, 109, 323 – 330, https://doi.org/https://doi.org/10.1016/j.cageo.2017.07.009, http://www.sciencedirect.com/science/article/pii/S0098300417307045, 2017.

Pearce, S., Ljubičić, R., Peña-Haro, S., Perks, M.~~T., Russell~~, Tauro, F., Pizarro, A.~~J., and Large, A.R. G.: Technical Note: Advances in flash flood monitoring using unmanned aerial vehicles (UAVs), Hydrology and Earth System Sciences, 20, 4005–4015, , 2016.~~ , Dal Sasso, S. F., Strelnikova, D., Grimaldi, S., Maddock, I., et al.: An Evaluation of Image Velocimetry Techniques under Low Flow Conditions and High Seeding Densities Using Unmanned Aerial Systems, Remote Sensing, 12, 232, 2020.

Perks, M.~~T.~~, Dal Sasso, S., Detert, M., Hauet, A., Jamieson, E., Le Coz, J., Pearce, S., Peña-Haro, S., Pizarro, A., Strelnikova, D., Tauro, F., Bomhof, J., Grimaldi, S., Goulet, A., Hortobágyi, B., Jodeau, M., ~~Le Coz, J.,~~ Käfer, S., Ljubičić, R., Maddock, I., Mayr, P., Paulus, G., Pénard, L., Sinclair, L., Vogel, U., and Manfreda, S.: Data on the harmonization of image velocimetry techniques, from ~~six~~ seven different countries, https://doi.org/10.4121/uuid:014d56f7-06dd-49ad-a48c-2282ab10428e, ~~, 2019.~~ http://doi.org/10.4121/uuid:014d56f7-06dd-49ad-a48c-2282ab10428e, 2020.

Perks, M. T., Russell, A. J., and Large, A. R. G.: Technical Note: Advances in flash flood monitoring using unmanned aerial vehicles (UAVs), Hydrology and Earth System Sciences, 20, 4005–4015, https://doi.org/10.5194/hess-20-4005-2016, 2016.

Pickering, C. J. D. and Halliwell, N. A.: Laser speckle photography and particle image velocimetry: photographic film noise, Appl. Opt., 23, 2961–2969, https://doi.org/10.1364/AO.23.002961, 1984.

Strelnikova, D., Paulus, G., Käfer, S., Anders, K.-H., Mayr, P., Mader, H., Scherling, U., and Schneeberger, R.: Drone-Based Optical Measurements of Heterogeneous Surface Velocity Fields around Fish Passages at Hydropower Dams, Remote Sensing, 12, https://doi.org/10.3390/rs12030384, 2020.

Sveen, J. K. and Cowen, E. A.: Quantitative imaging techniques and their application to wavy flows, pp. 1–49, https://doi.org/10.1142/9789812796615_0001, 2004.

Tauro, F. and Grimaldi, S.: Ice dices for monitoring stream surface velocity, Journal of Hydro-environment Research, 14, 143 – 149, https://doi.org/https://doi.org/10.1016/j.jher.2016.09.001, 2017.

Tauro, F., Porfiri, M., and Grimaldi, S.: Orienting the camera and firing lasers to enhance large scale particle image velocimetry for streamflow monitoring, Water Resources Research, 50, 7470–7483, https://doi.org/10.1002/2014WR015952, 2014.

Tauro, F., Petroselli, A., Porfiri, M., Giandomenico, L., Bernardi, G., Mele, F., Spina, D., and Grimaldi, S.: A novel permanent gauge-cam station for surface-flow observations on the Tiber River, Geoscientific Instrumentation, Methods and Data Systems, 5, 241–251, https://doi.org/10.5194/gi-5-241-2016, 2016a.

Tauro, F., Porfiri, M., and Grimaldi, S.: Surface flow measurements from drones, Journal of Hydrology, 540, 240 – 245, https://doi.org/https://doi.org/10.1016/j.jhydrol.2016.06.012, 2016b.

Tauro, F., Piscopia, R., and Grimaldi, S.: Streamflow Observations From Cameras: Large-Scale Particle Image Velocimetry or Particle Tracking Velocimetry?, Water Resources Research, 53, 10 374–10 394, https://doi.org/10.1002/2017WR020848, 2017.

Tauro, F., Selker, J., van de Giesen, N., Abrate, T., Uijlenhoet, R., Porfiri, M., Manfreda, S., Caylor, K., Moramarco, T., Benveniste, J., Ciraolo, G., Estes, L., Domeneghetti, A., Perks, M. T., Corbari, C., Rabiei, E., Ravazzani, G., Bogena, H., Harfouche, A., Brocca, L., Maltese, A., Wickert, A., Tarpanelli, A., Good, S., Alcala, J. M. L., Petroselli, A., Cudennec, C., Blume, T., Hut, R., and Grimaldi, S.: Measurements and Observations in the XXI century (MOXXI): innovation and multi-disciplinarity to sense the hydrological cycle, Hydrological Sciences Journal, 63, 169–196, https://doi.org/10.1080/02626667.2017.1420191, 2018a.

Tauro, F., Tosi, F., Mattoccia, S., Toth, E., Piscopia, R., and Grimaldi, S.: Optical Tracking Velocimetry (OTV): Leveraging Optical Flow and Trajectory-Based Filtering for Surface Streamflow Observations, Remote Sensing, 10, https://doi.org/10.3390/rs10122010, https://www.mdpi.com/2072-4292/10/12/2010, 2018b.

Tauro, F., Piscopia, R., and Grimaldi, S.: PTV-Stream: A simplified particle tracking velocimetry framework for stream surface flow monitoring, CATENA, 172, 378 – 386, https://doi.org/https://doi.org/10.1016/j.catena.2018.09.009, http://www.sciencedirect.com/science/article/pii/S0341816218303771, 2019.

Thielicke, W. and Stamhuis, E.: PIVlab – Towards User-friendly, Affordable and Accurate Digital Particle Image Velocimetry in MATLAB, Journal of Open Research Software, 2, e30, http://doi.org/10.5334/jors.bl, 2014.

Tsubaki, R.: LSPIV app, https://sites.google.com/site/rtsubaki/lspiv-app, 2018.